Supporting Information for:

Synthesis of 5,10,15,20-tetraarylporphyrins and Their Platinum (II) Complexes as Luminescent Oxygen Sensing Materials

Wenting Wu,[a] Wanhua Wu,[a] Shaomin Ji,[a] Huimin Guo,[b] Xin Wang[c] and Jianzhang Zhao[a]*

[a] *State Key Laboratory of Fine Chemicals, School of Chemical Engineering, Dalian University of Technology, 158 Zhongshan Road, Dalian 116012 P.R. China*

[b] *Department of Chemistry, School of Chemical Engineering, Dalian University of Technology, 158 Zhongshan Road, Dalian 116012 P.R. China*

[c] *Faculty of Chemistry, Sichuan University, Chengdu 610064, P. R. China*

Email: zhaojzh@dlut.edu.cn

Index

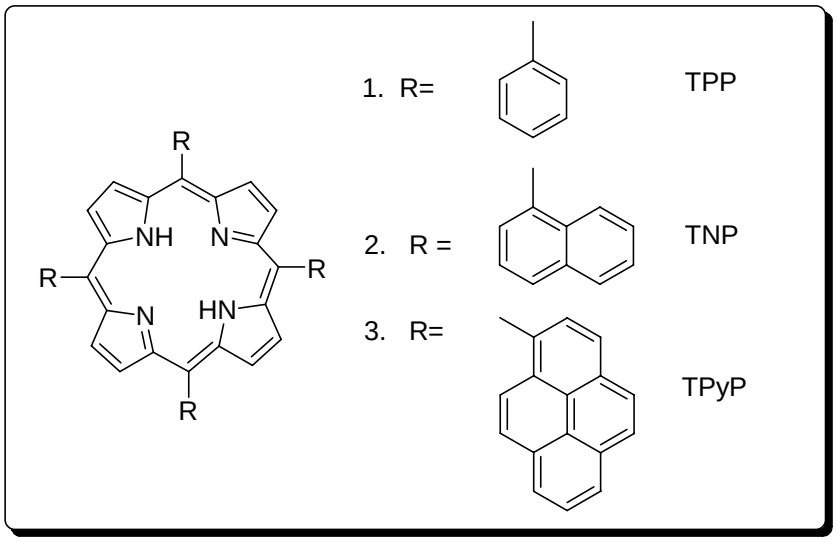

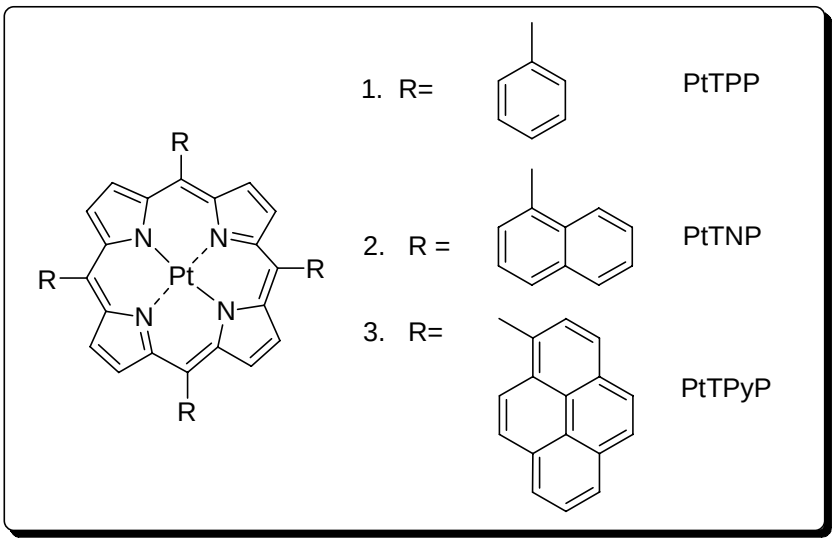

Experimental Section

General

The ground state structure of complexes were optimized using density functional theory (DFT)[1] with B3LYP functional and 6-31G(d)/ LanL2DZ basis set. The excited state related calculations were carried out with the Time dependent density functional theory (TD-DFT) with the optimized structure of the ground state (DFT 6-31G(d)/ LanL2DZ) There are no imaginary frequencies in frequency analysis of all calculated structures, therefore each calculated structure express an energy minimum. All these calculations were performed in GAUSSIAN03 suit.[2]

Reference:

1. Hohenberg P, Kohn W. *Phys. Rev.* 1964; **136**: B864.

2. Gaussian 03, Revision D.01. M. J. Frisch, G. W. Trucks, H. B. Schlegel, G. E. Scuseria, M. A. Robb, J. R.Cheeseman, Jr., J. A. Montgomery, T. Vreven, K. N. Kudin, J.C. Burant, J.M. Millam, S. S. Iyengar, J. Tomasi, V. Barone, B. Mennucci, M. Cossi, G. Scalmani, N. Rega, G. A. Petersson, H. Nakatsuji, M. Hada, M. Ehara, K. Toyota, R. Fukuda, J. Hasegawa, M. Ishida, T. Nakajima, Y. Honda, O. Kitao, H. Nakai, M. Klene, X. Li, J. E. Knox, H. P. Hratchian, J. B. Cross, C. Adamo, J. Jaramillo, R.

Gomperts, R. E. Stratmann, O. Yazyev, A. J. Austin, R. Cammi, C. Pomelli, J.W. Ochterski, P.Y. Ayala, K. Morokuma, G.A. Voth, P. Salvador, J.J. Dannenberg, V.G. Zakrzewski, S. Dapprich, A. D. Daniels, M.C. Strain, O. Farkas, D.K. Malick, A.D. Rabuck, K. Raghavachari, J.B. Foresman, J.V. Ortiz, Q. Cui, A.G. Baboul, S. Clifford, J. Cioslowski, B.B. Stefanov, G. Liu, A. Liashenko, P. Piskorz, I. Komaromi, R.L. Martin, D.J. Fox, T. Keith, M.A. Al-Laham, C.Y. Peng, A. Nanayakkara, M. Challacombe, P.M.W. Gill, B. Johnson, W. Chen, M.W. Wong, C. Gonzalez, J.A. Pople, Gaussian, Inc., Willingford, **2004**

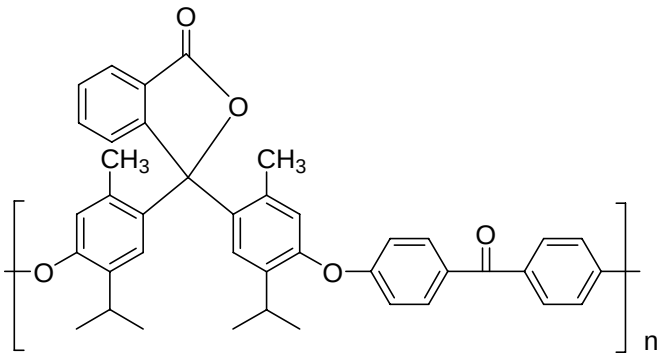

Scheme S1. Structure of polymer IMPEK-C.

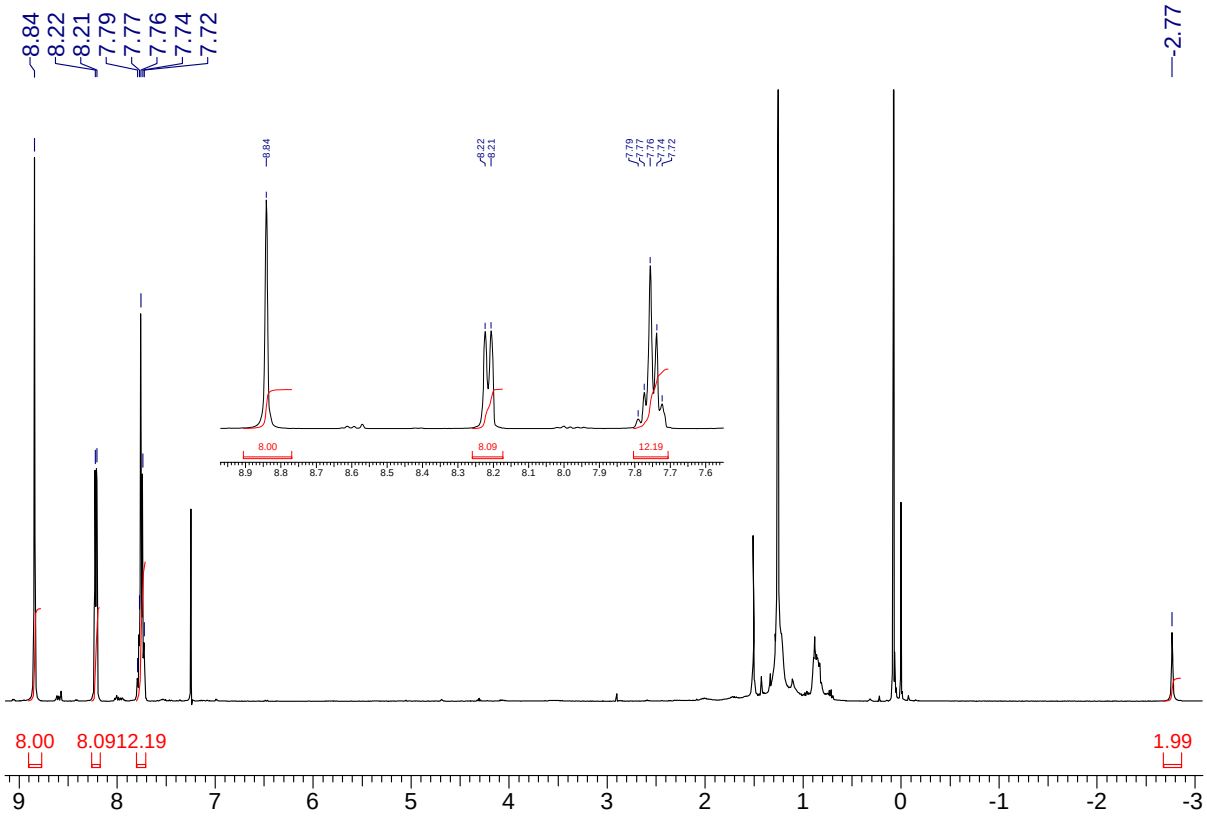

Figure S1. ^{1}H NMR of **TPP** ($CDCl_3$, 400 MHz)

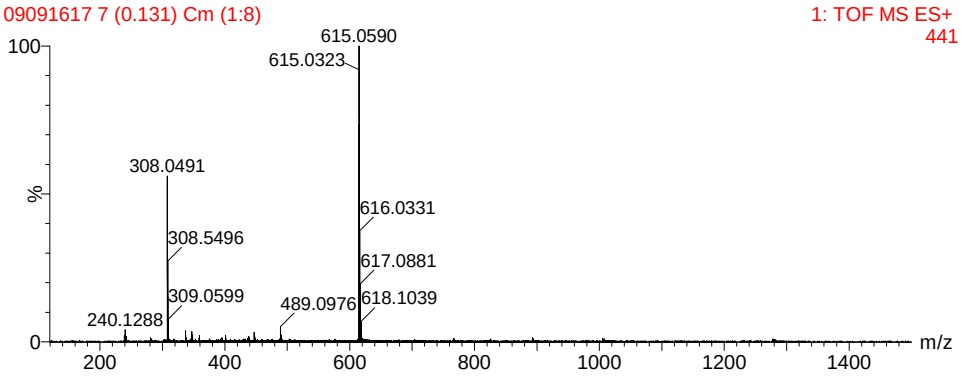

Figure S2. TOF MS (ESI) of **TPP.**

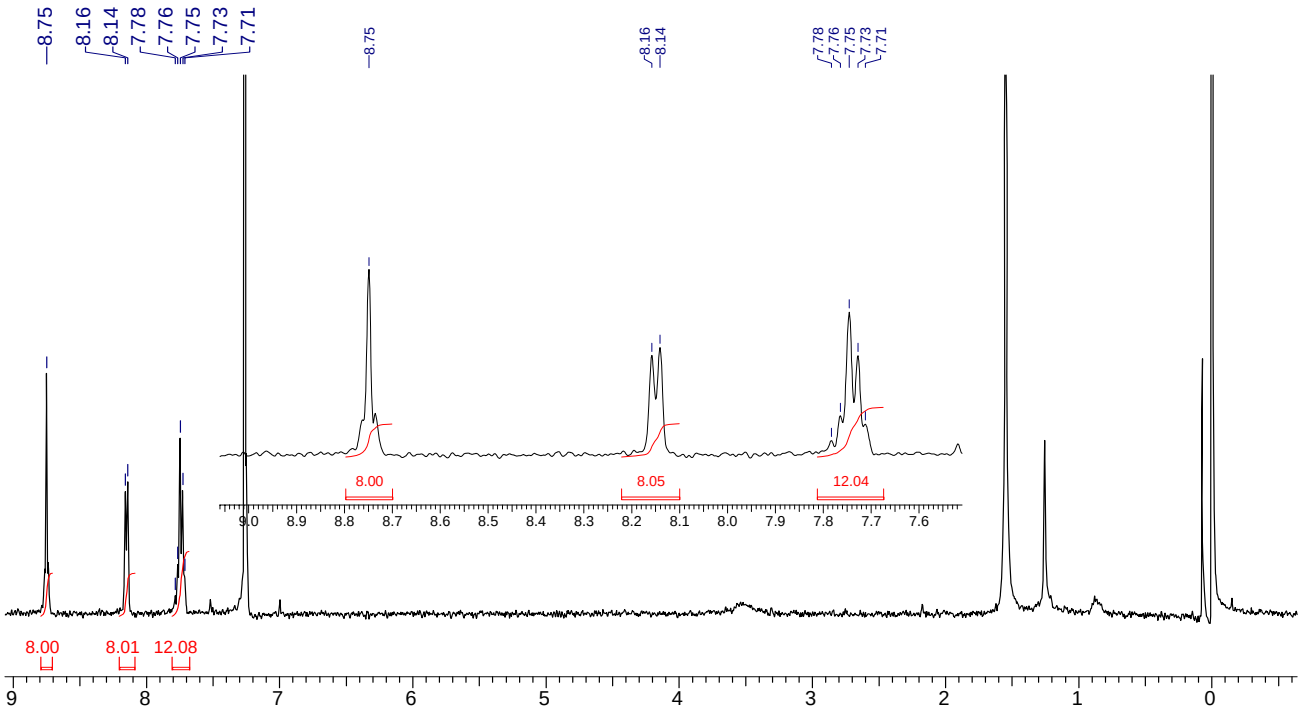

Figure S3. ^{1}H NMR of **Pt-TPP** ($CDCl_3$, 400 MHz)

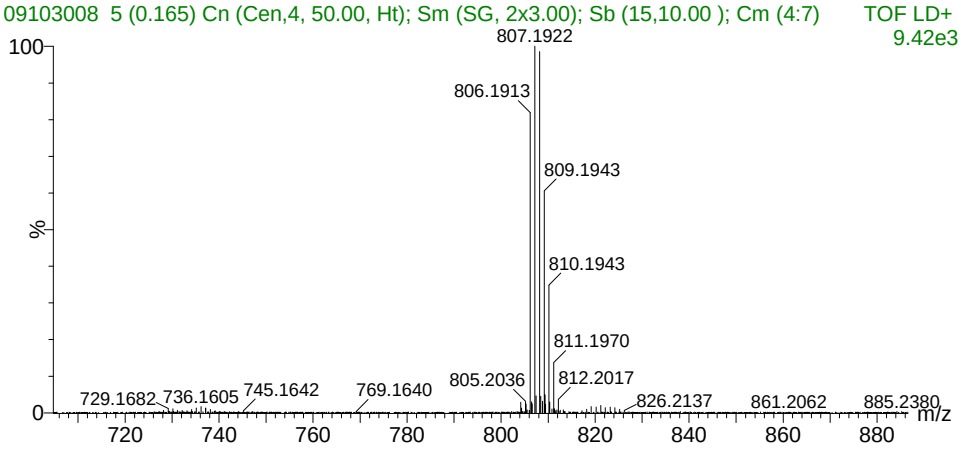

Figure S4. MALDI MS of **PtTPP.**

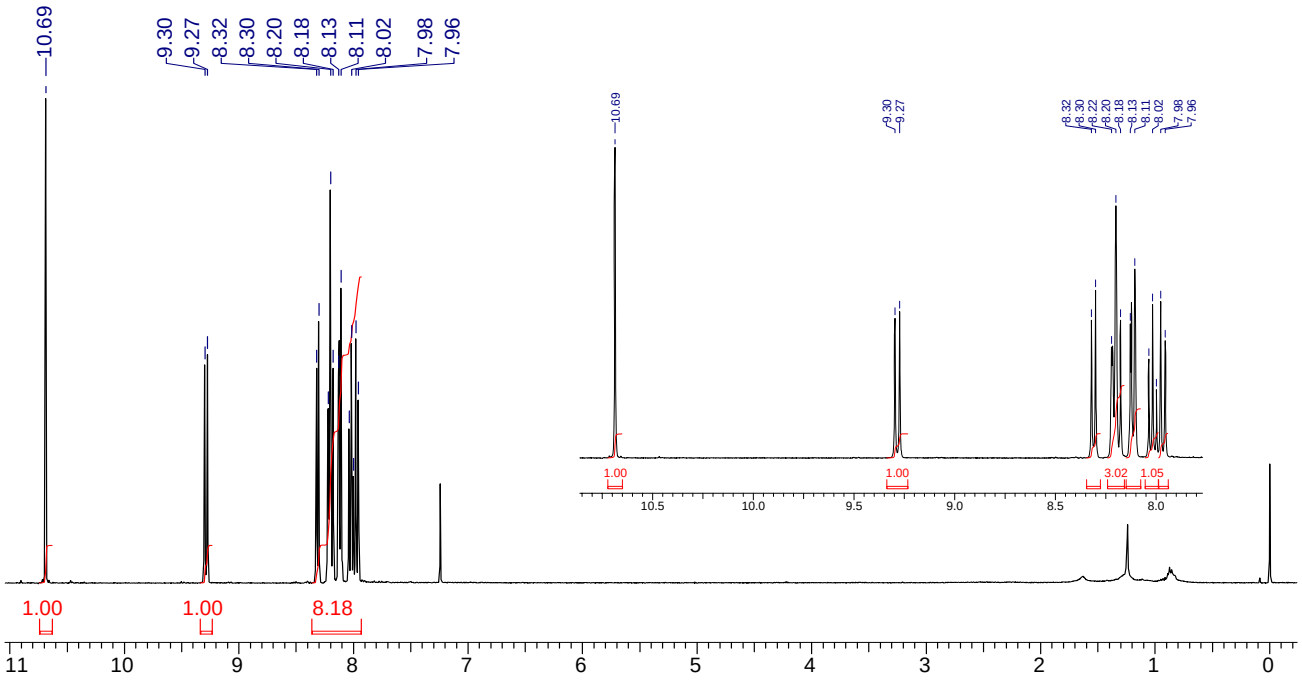

Figure S5. ^{1}H NMR of **pyrene-1-carbaldehyde** ($CDCl_3$, 400 MHz).

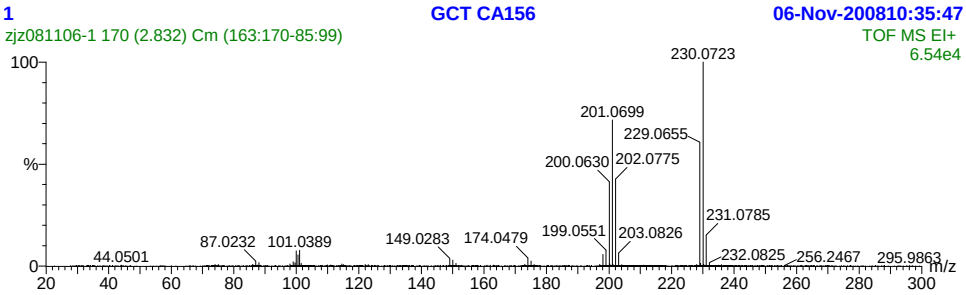

Figure S6. TOF ESI MS of **pyrene-1-carbaldehyde.**

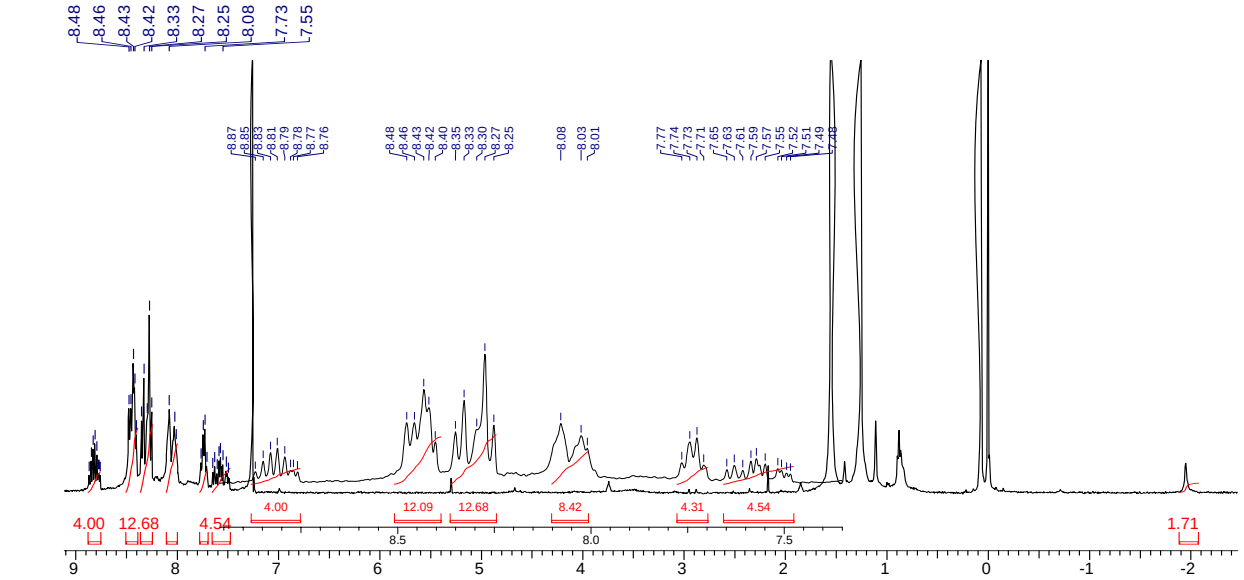

Figure S7. ^{1}H NMR of **TPyP** ($CDCl_3$, 400 MHz).

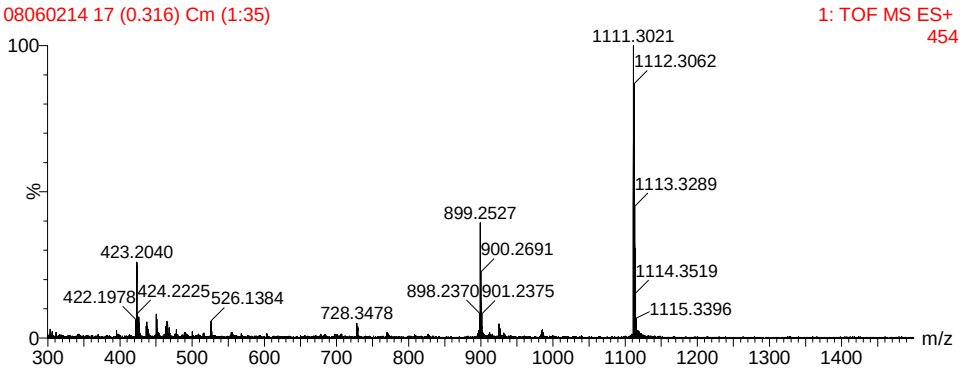

Figure S8. TOF ESI MS of **TPyP.**

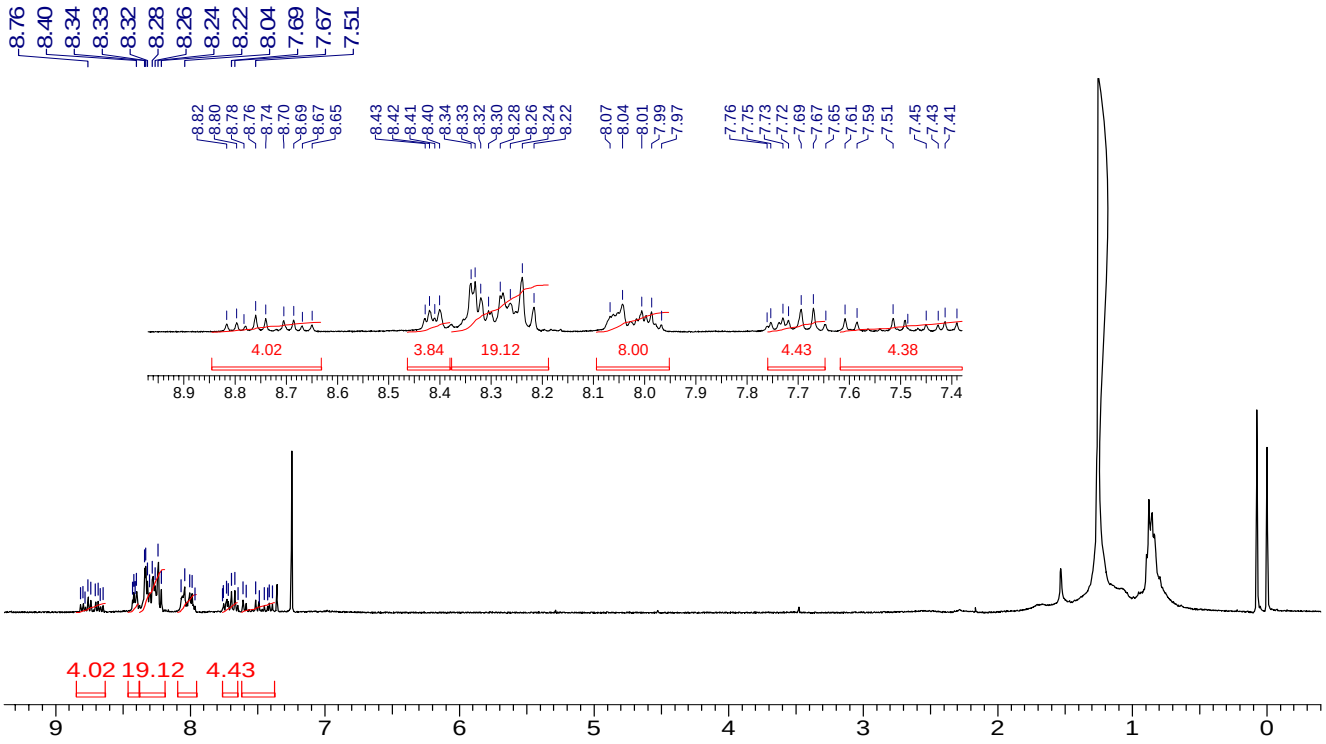

Figure S9. ^{1}H NMR of **Pt-PyP** ($CDCl_3$, 400 MHz).

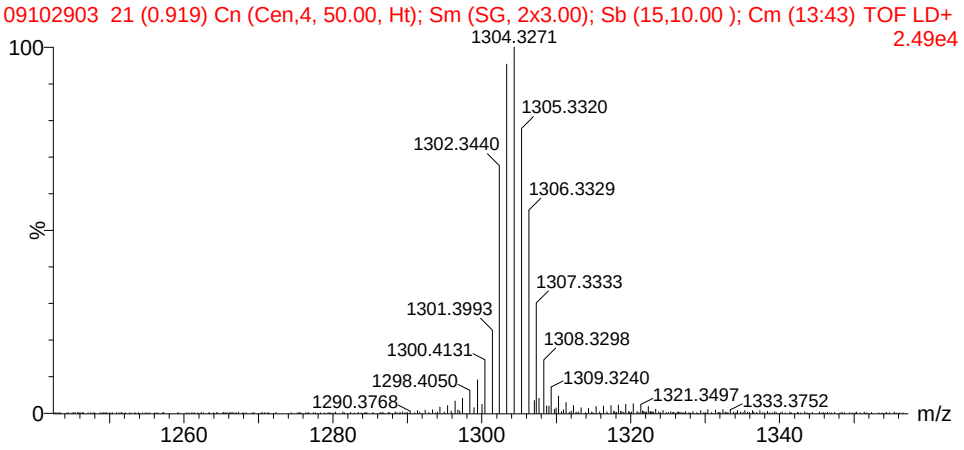

Figure S10. MALDI MS of **Pt-PyP.**

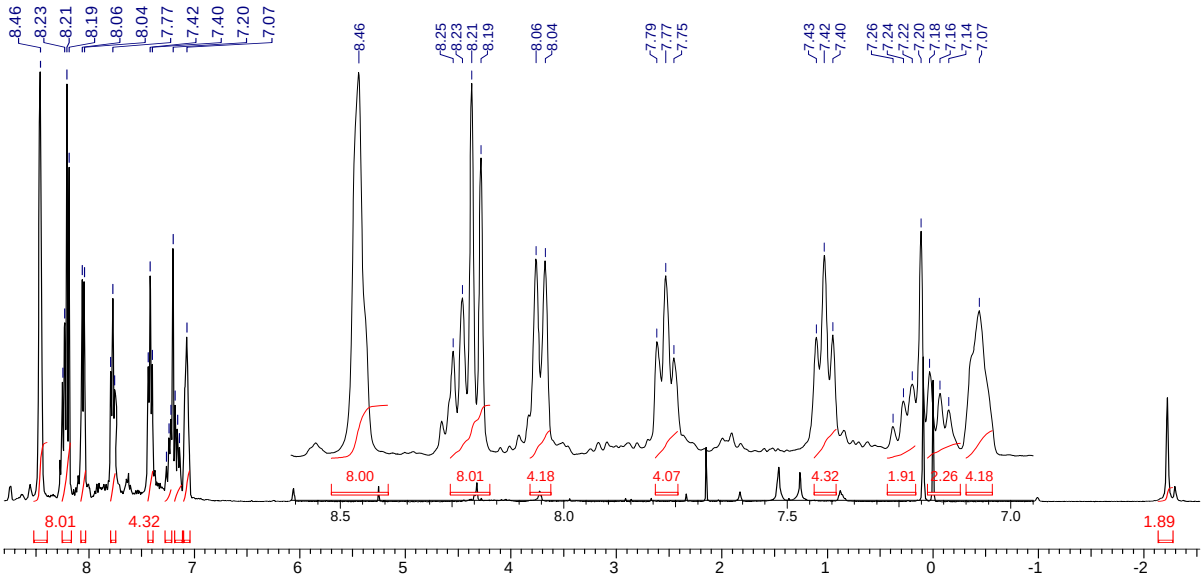

Figure S11. ^{1}H NMR of **TNP** ($CDCl_3$, 400 MHz).

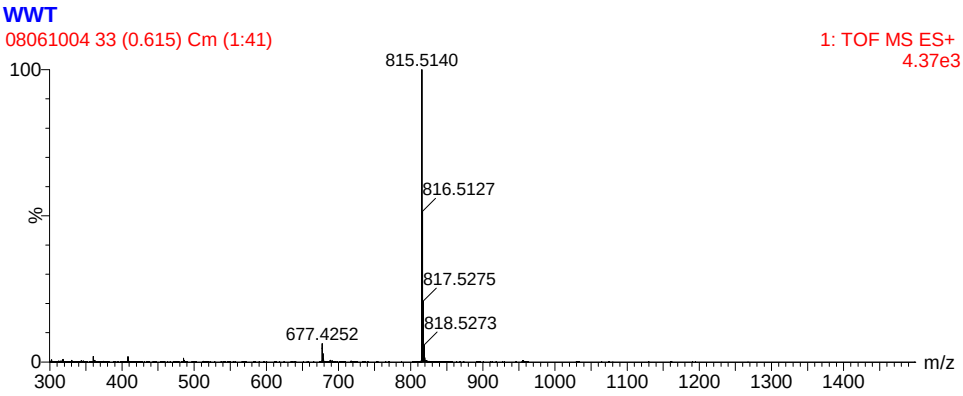

Figure S12. TOF ESI MS of **TNP.**

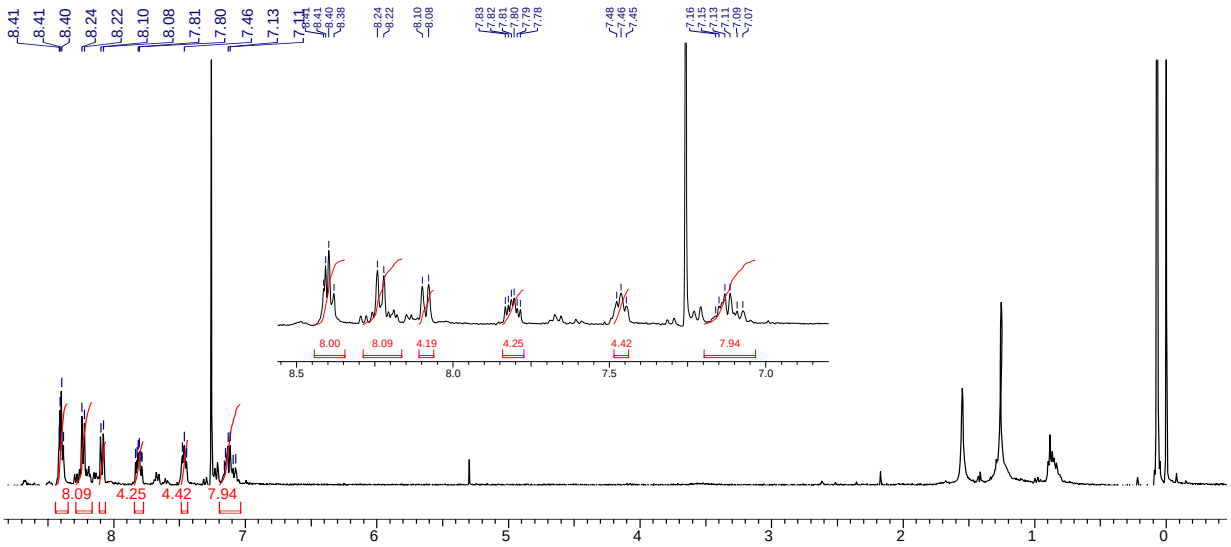

Figure S13. ^{1}H NMR of **Pt-TNP** ($CDCl_3$, 400 MHz).

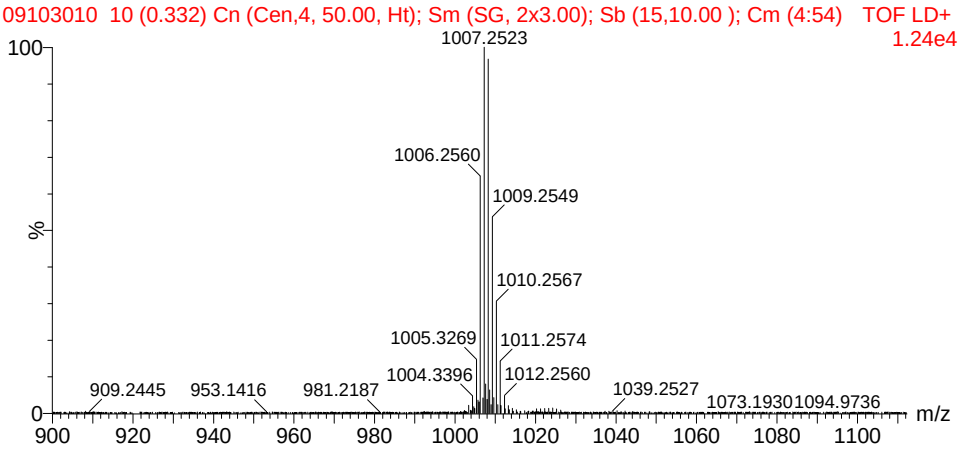

Figure S14. MALDI MS of **Pt-TNP.**

Table S1. Selected Electronic Excitation Energies (eV) and Corresponding Oscillator Strengths (*f*), Main Configurations and CI Coefficients of the Low-lying Electronically Excited States of **TNP,** Calculated by TDDFT//B3LYP/6-31G(d), Based on the DFT//B3LYP/6-31G(d) Optimized Ground State Geometries.

	Electronic transition	**TDDFT//B3LYP/6-31G(d)**				
		Energy (eV) [a]	***f*** [b]	**Composition** [c]	**CI** [d]	**character**
Singlet						
	$S_0 \rightarrow S_1$	2.18 eV 568 nm	0.0054	H-1→L	0.46655	LC
				H→L+1	0.55609	LC
	$S_0 \rightarrow S_2$	2.34 eV 531 nm	0.0099	H-1→L+1	-0.47613	LC
				H→L	0.52030	LC
	$S_0 \rightarrow S_3$	3.02 eV 411 nm	0.2696	H-5→L	0.35836	LC
				H-2→L+1	0.41241	LC
				H-1→L	-0.29916	LC
	$S_0 \rightarrow S_7$	3.12 eV 377 nm	0.3868	H-5→L+1	0.47112	
				H-2→L	-0.34824	LC
				H-1→L+1	-0.26127	LC
				H→L	-0.20405	LC
Triplet						
	$S_0 \rightarrow T_1$	1.39 eV 891 nm	0.0000	H−1→L+1	-0.39293	LC
				H→L	0.78767	LC
	$S_0 \rightarrow T_2$	1.72 eV 719 nm	0.0000	H-1→L	0.17639	LC
				H→L+1	0.76702	LC
	$S_0 \rightarrow T_3$	1.96 eV 631 nm	0.0000	H-1→L+1	0.69977	LC
				H→L	0.25577	LC
	$S_0 \rightarrow T_4$	1.99 eV 622 nm	0.0000	H-1→L	0.73377	LC

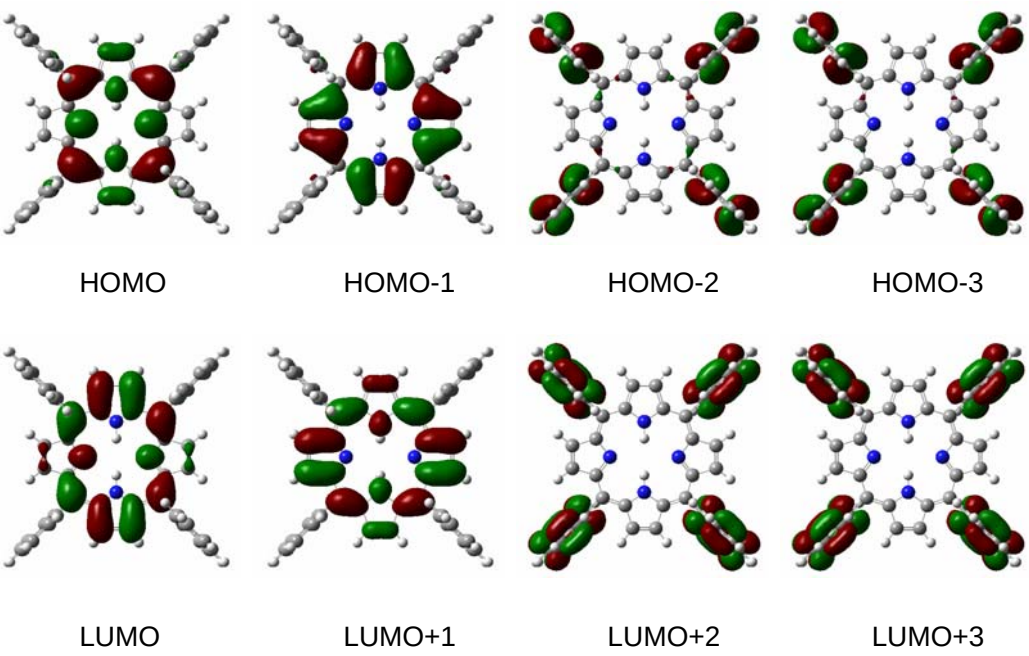

Scheme S2. Qualitative scheme of frontier molecular orbitals of the ligand of **TNP** calculated by DFT/TDDFT at the B3LYP/6-31G((d)/ LanL2DZ level using Gaussian 03.

Table S2. Selected Electronic Excitation Energies (eV) and Corresponding Oscillator Strengths (*f*), Main Configurations and CI Coefficients of the Low-lying Electronically Excited States of **Pt-TNP,** Calculated by TDDFT//B3LYP/6-31G(d), Based on the DFT//B3LYP/6-31G(d) Optimized Ground State Geometries.

	Electronic transition	**TDDFT//B3LYP/6-31G(d)**				
		Energy (eV) [a]	***f*** [b]	**Composition** [c]	**CI** [d]	**character**
Singlet	$S_0 \rightarrow S_1$	2.50 eV 495 nm	0.0026	H-1→L+1	0.48102	LC&LMCT
				H→L	0.52998	LC&LMCT
	$S_0 \rightarrow S_2$	2.55 eV 495 nm	0.0026	H-1→L	0.48113	LC&LMCT
				H→L+1	0.52989	LC&LMCT
	$S_0 \rightarrow S_7$	3.17 eV 391 nm	0.1423	H-7→L+1	0.36758	
				H-4→L	0.50505	
				H-1→L	0.20467	LC&LMCT
				H→L+1	0.19043	LC&LMCT
	$S_0 \rightarrow S_8$	3.17 eV 391 nm	0.1373	H-7→L	0.37105	
				H-4→L+1	0.50591	
				H-1→L+1	0.20046	LC&LMCT
				H→L	0.18761	LC&LMCT
	$S_0 \rightarrow S_{11}$	3.25 eV 382 nm	0.3187	H-7→L	0.36103	
				H-4→L+1	0.48853	
				H-1→L+1	0.22462	LC&LMCT
				H→L	0.20763	LC&LMCT
	$S_0 \rightarrow S_{12}$	3.25 eV 382 nm	0.3112	H-7→L+1	0.36494	
				H-4→L	0.48985	
				H-1→L	0.22002	LC&LMCT
				H→L+1	0.20475	LC&LMCT
	$S_0 \rightarrow S_{17}$	3.40 eV 365 nm	0.6995	H-7→L	0.47291	
				H-1→L+1	0.30310	LC&LMCT
				H→L	0.25344	LC&LMCT
	$S_0 \rightarrow S_{18}$	3.40 eV 365 nm	0.6993	H-7→L+1	0.47261	
				H-1→L	0.30349	LC&LMCT
	$S_0 \rightarrow S_{27}$	3.91 eV 317 nm	0.1042	H-13→L	0.26598	
				H-9→L	0.62276	
	$S_0 \rightarrow S_{28}$	3.91 eV 317 nm	0.1040	H-13→L+1	0.26432	
				H-9→L+1	0.62343	
Triplet	$S_0 \rightarrow T_1$	1.91 eV 650 nm	0.0000	H-1→L+1	0.63326	LC&LMCT
				H→L	-0.48651	LC&LMCT
	$S_0 \rightarrow T_2$	1.91 eV 650 nm	0.0000	H-1→L	0.63361	LC&LMCT
				H→L+1	0.48597	LC&LMCT
	$S_0 \rightarrow T_3$	2.16 eV 574 nm	0.0000	H-1→L+1	0.44917	LC&LMCT
				H→L	0.57651	LC&LMCT
	$S_0 \rightarrow T_4$	2.16 eV 574 nm	0.0000	H-1→L	-0.44862	LC&LMCT

H→L+1		0.57691	LC&LMCT

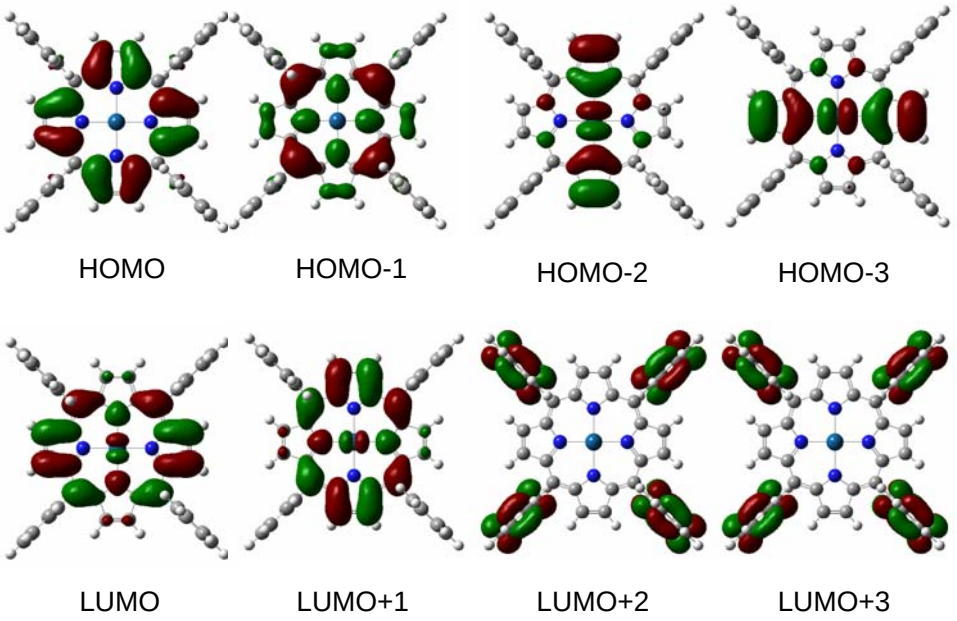

Scheme S3. Qualitative scheme of frontier molecular orbitals of the ligand of **Pt-TNP** calculated by DFT/TDDFT at the B3LYP/6-31G((d)/ LanL2DZ level using Gaussian 03.

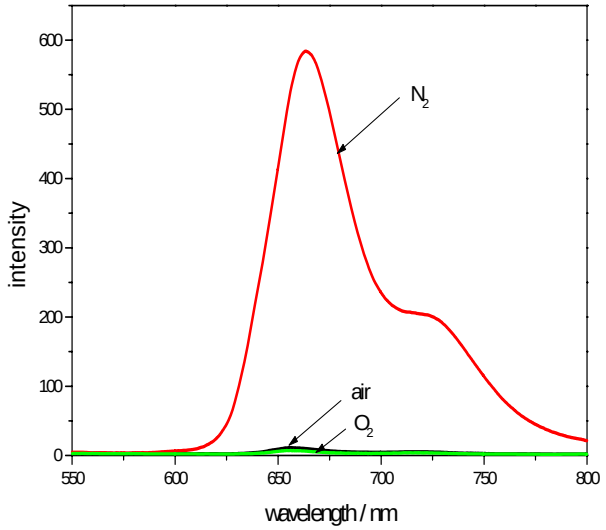

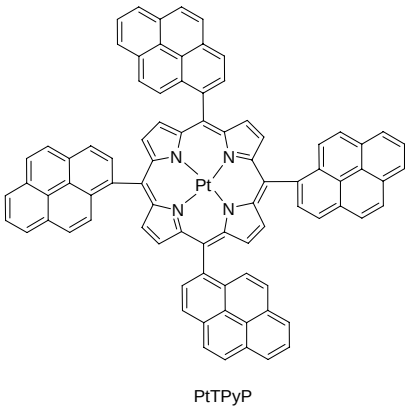

PtTPyP

Figure S15. Room-temperature emission spectra of complex **Pt-TPyP** under nitrogen, air and O_2 atmosphere. λ_{ex} = 432 nm, 2×10^{-6} mol/L complexes solution in $CHCl_3$.

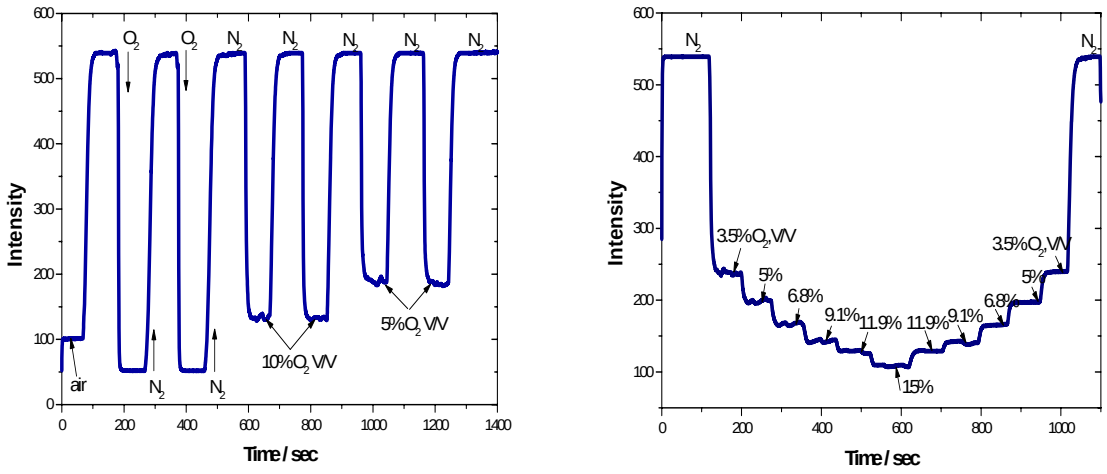

Figure S16. Phosphorescent intensity response of sensing films of the complex **Pt-TPyP** in IMPES-C. a) Emission intensity response to O_2/N_2 saturation cycles; b) Emission intensity response to step variations of O_2 concentrations. λ_{ex}= 433 nm, λ_{em} = 633 nm. Measured with home assembled optical fiber/flow cell system.

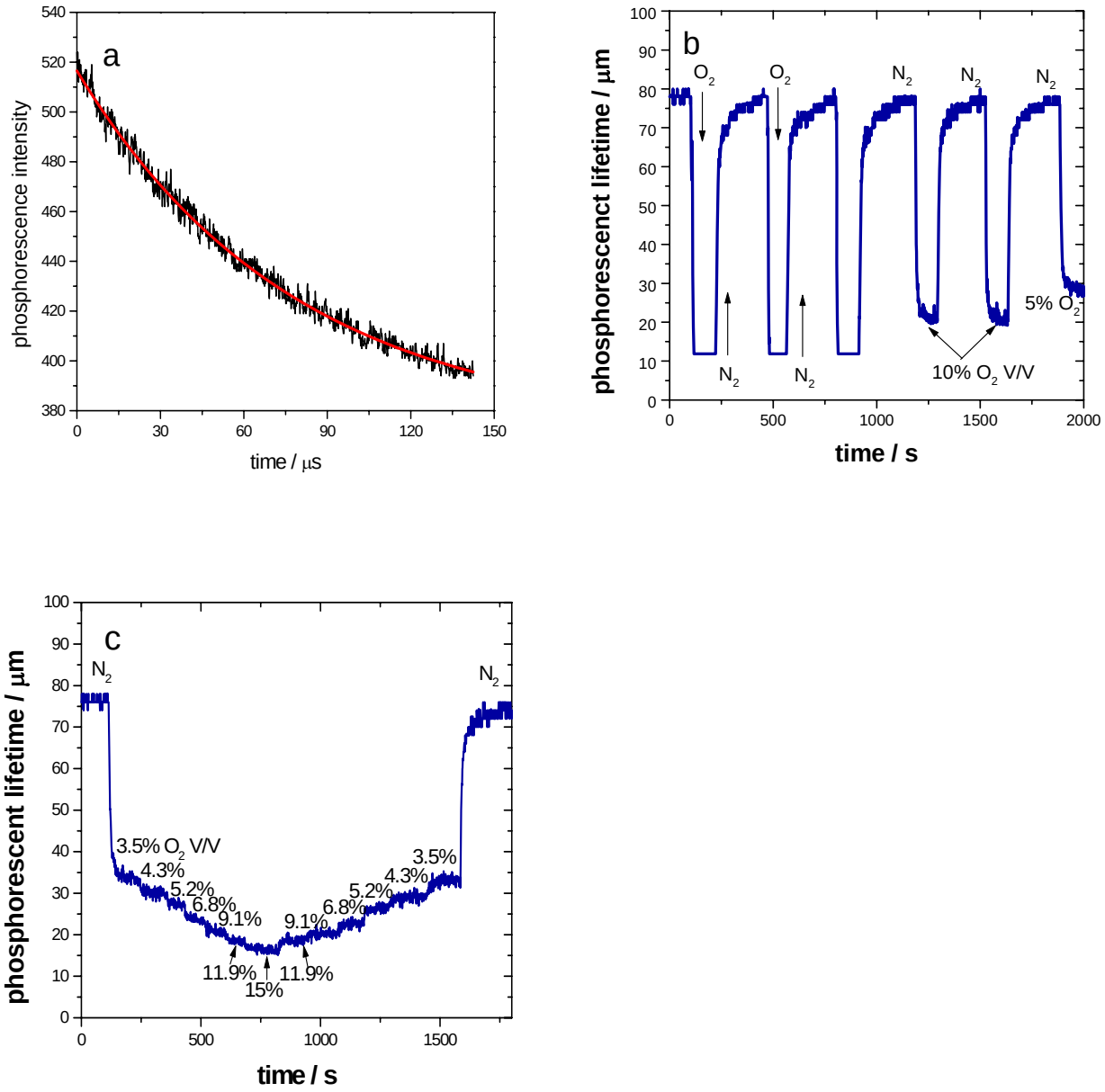

Figure S17. Oxygen sensing property of the Pt-TNP polymer films monitored by the luminescence lifetime variation against the oxygen partial pressure changes. (a) phosphosrescence decay curve of PtTNP in IMPEK-C in neat N_2, Monoexponential decay regression gave lifetime τ = 78.1±0.6 μs (r^2 = 0.99). (b) phosphorescence lifetime response of sensing film of Pt-TNP in IMPEK-C to O_2/N_2 saturation cycles and switch between neat N_2, 10%O_2 and 5%O_2 (V / V). (513 nm LED as excitation light source and the emission beyond 600 nm is used for the τ monitoring). (c) lifetime response of sensing film of Pt-TNP in IMPEK-C to step variation of O_2 concentration in O_2/N_2 mixture.

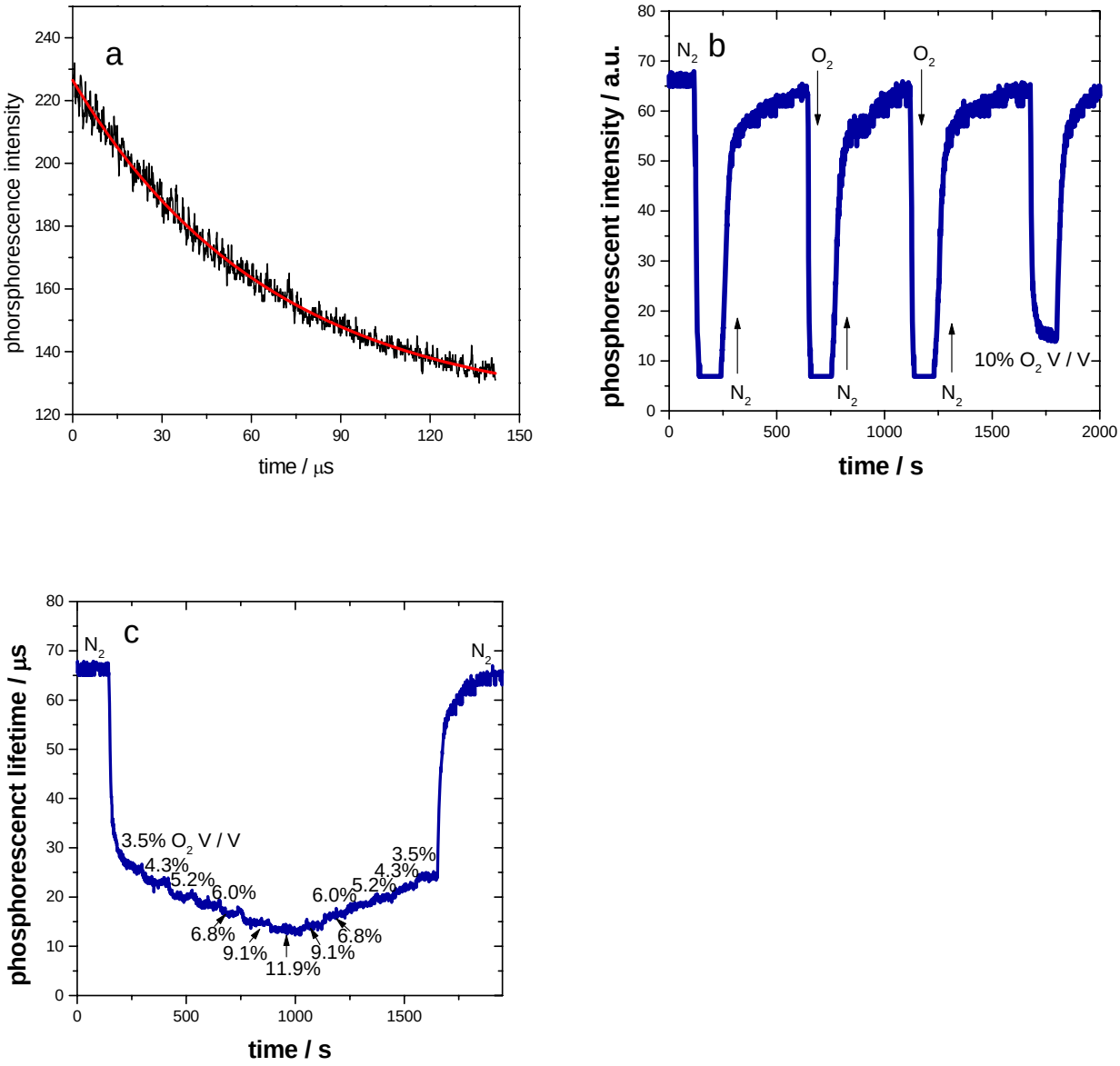

Figure S18. Oxygen sensing property of the Pt-TPyP polymer films monitored by the luminescence lifetime variation against the oxygen partial pressure changes. (a) phosphosrescence decay curve of Pt-TPyP in IMPEK-C in neat N_2, Monoexponential decay regression gave lifetime τ = 66.7±0.9 μs (r^2 = 0.99). (b) phosphorescence lifetime response of sensing film of Pt-TPyP in IMPEK-C to O_2/N_2 saturation cycles and switch between neat N_2, 10%O_2 (V / V). (513 nm LED as excitation light source and the emission beyond 600 nm is used for the τ monitoring). (c) lifetime response of sensing film of Pt-TPyP in IMPEK-C to step variation of O_2 concentration in O_2/N_2 mixture.

End of the Supporting Information.